# Finite Element Analysis and Modeling of Details Timber Structure

O. Sucharda, D. Mikolasek, J. Brozovsky

***Abstract*—**The paper analyses a timber hall. A beam model is globally analysed and focus is placed on structural details. 3D computational models are used for the analysis of the structural models. Nonlinearities are taken into account. A particular attention is paid to the analysis of the top steel joint with pins. The objective of the paper is to evaluate stiffness of some details for a glue timber lam structure. For that purpose, the nonlinear models of materials, geometric nonlinearities and contact elements are utilised. The software used for modelling is based on the Finite Element Method.

***Keywords*—**beam, 3D finite elements, computational model, timber, detail, contact elements, analysis

## I. Introduction

TIMBER ranks among the modern materials. It is used in many structural elements in the building industry. Design procedures are described in [1] and [2]. There are, however, certain disadvantages in the use of timber and such disadvantages should be considered when preparing advanced structural designs. Timber is often combined with other materials [3]. For instance, CFRP [4] is used for additional adaptations [5]. The Finite Element Method and orthotropic material models of timber are used in design [6] a [7]. Another method used for analyses of the steel structures is the Finite Element Method [8] and [9].

For those reasons, a particular attention is paid to research and assessment of the structures [10]. For some structures it is advisable to consider the stochastic nature of input data as in [11] and [12] or to use another suitable probabilistic method [13]. A recommendation for design of timber structures shows [14], [15], [16] and [17]. It is also important to calculate the testing wooden elements and details [18], [19] and [20].

The paper focuses on the numerical modelling and analysis of steel joints in the glue lam timber structure. The main purpose of the paper is to describe and evaluate deformation at contact surfaces between the timber part of the structure and steel fasteners.

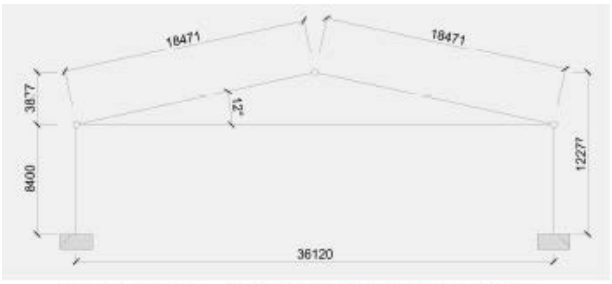


Fig. 1 Frame – the typical bay in the structure

## II. Hall structure

The structural segments of the timber structure have been chosen in a global analysis pursuant to standardised procedures described in the EC [1] and [2]. A beam computation model in the SCIA [21] has been used. The program is based on the Finite Element Method [22]. Below described are the combinations which have been chosen in order to analyse the details.

A particular attention has been paid to the transfer of external load into the structure and external joints and to impacts of such transfer. Fig. 1 shows the transversal frame of the structure. The analysed structure is a sport hall with the ground plan of ca. 37 x 44.8 m. The height in the roof ridge is 13.57 m. The axial distance between the bays is 5.60 m and 8.40 m high columns are fixed along the perimeter of the hall. The double-pitch roof is inclined at ca. 12°. The frame consists of glue lam timber beams, 1300 x 200 mm, made from GL28c lamellas.

| Load Combination | $H_x$ [kN] | $V_z$ [kN] | $M_y$ [kNm] | $M_z$ [kNm] |
|---|---|---|---|---|
| NC41 | -685.52 | 2.51 | 0.11 | 0.02 |
| NC57 | -360.69 | 40.80 | -0.74 | -0.16 |

Table 1 Forces in top connections – the beam model

At the top, the frame is connected via a steel joint (welded steel elements, S355). In the footing, the frame is connected via a steel tie, S355 dia. 55 mm, Fig. 2 shows the beam model

Acknowledgements: This outcome has been achieved with the financial support of the Ministry of Education, Youth and Sports of the Czech Republic with use of the Institutional support of conceptual development of research in 2014.

Oldrich Sucharda, VSB-Technical University of Ostrava, Faculty of Civil Engineering, Department of Structural Mechanics, L. Podeště 1875, 708 33 Ostrava, Czech Republic (phone: +420597321391; e-mail: oldrich.sucharda@vsb.cz).

David Mikolasek, VSB-Technical University of Ostrava, Faculty of Civil Engineering, Department of Structural Mechanics, L. Podeště 1875, 708 33 Ostrava, Czech Republic (phone: +420597321391; e-mail: david.mikolasek@vsb.cz).

Jiri Brozovsky, VSB-Technical University of Ostrava, Faculty of Civil Engineering, Department of Structural Mechanics, L. Podeště 1875, 708 33 Ostrava, Czech Republic (phone: +420597321321; e-mail: jiri.brozovsky@vsb.cz).

of the hall.

The system (the glued beams and steel joints which form a triangle) is placed on fixed columns made from reinforced concrete. 3D stability of the load-carrying roof structure is ensured by steel drawn crosses at the level of the roof. The crosses are connected to the columns and lead, through the reinforced eaves edge, to the gable wall. The beams are located at column heads. The most relevant combinations, NC41 and NC57, have been chosen from among the standardised methods for the analyses of details. Table 1 shows results. Fig. 3 and 4 show the loading.

NC41 in Fig. 3 results in the maximum tension in the steel tie and the maximum compression in the top connection with the horizontal force - $H_x$. NC57 in Fig. 4 results in the maximum vertical force $V_z$ in the top joint (this load causes the top joint to rotate).

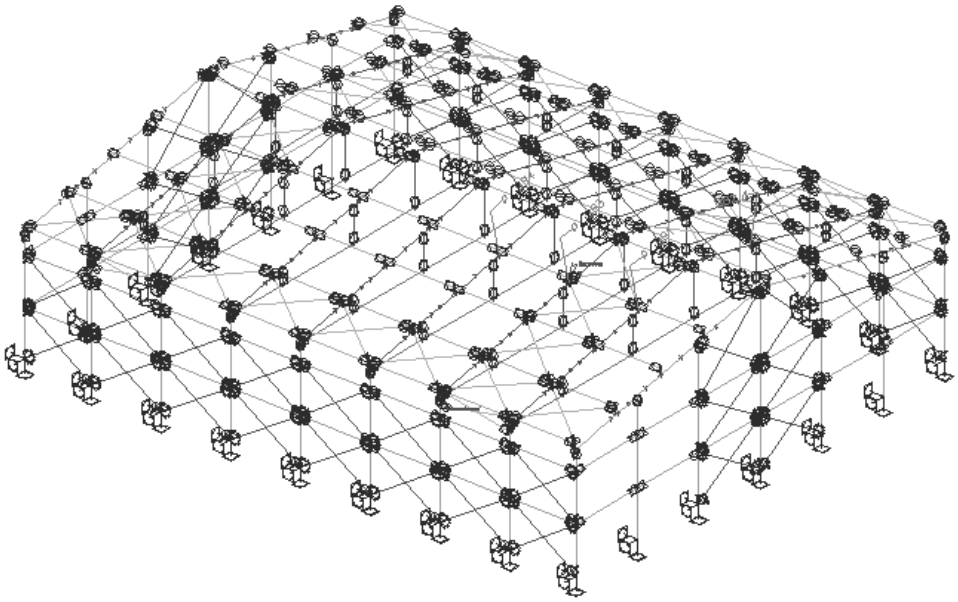

Fig. 2 Geometry and external bonds in the 3D beam model of the hall – the beam model

The hall structure was loaded in line with EC (snow load - ČSN EN 1991-1-3:2005/Z1:2006 and wind load ČSN EN 1991-1-4:2007, building structure load is assumed pursuant to ČSN EN 1991-1-1:2004). In case of the timber structure, the design was based on ČSN 73 1702 mod DIN 1052:2004. The reason for choosing ČSN 73 1702 mod DIN 1052:2004 as the basis for evaluation of segments of the timber structure is that the standard is based on the German standard DIN 1052 which describes very well the approach to issues which occur in practical design of timber structures.

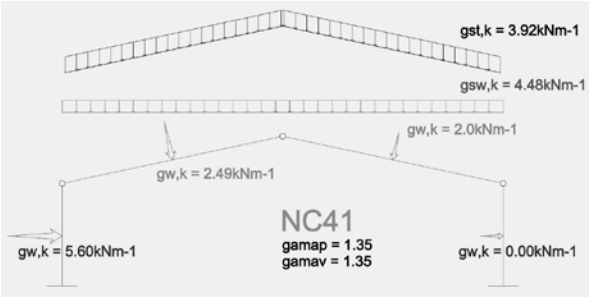


Fig. 3 SCIA – the loading condition NC41

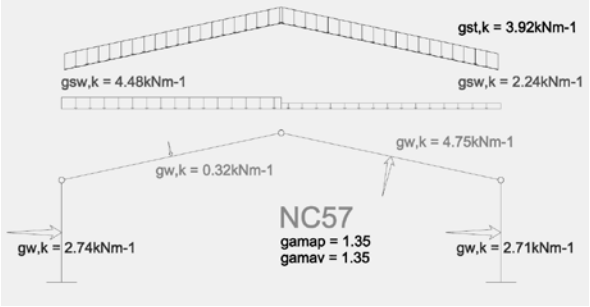


Fig. 4 SCIA – the loading condition NC57

## III. HALL STRUCTURE

The model has been created in ANSYS [23]. As the model would need too much time for calculation, the task has been simplified and a plain bay has been used.

Such simplification is advisable because it is rather easy to enter boundary conditions and loads in nodes. Because there is no bond which would be normal to the soft plane of the frame, non-shifting external bonds are used in places of supports. In the real structure, they make the plane rigid in bracing fields and, in turn, in foundations and gable wall.

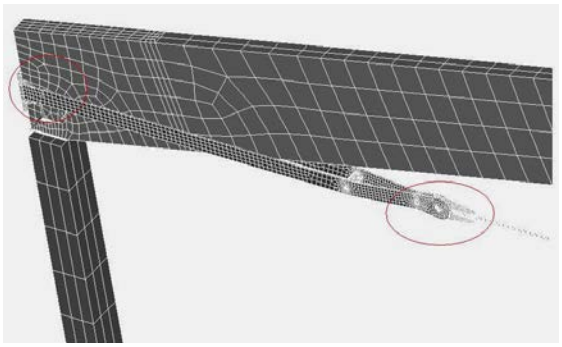

Fig. 5 Detail of the finite element grid: the tie + glue lam timber structure

The segments above shows details of the tie connection in the 3D model. It shows how the steel elements are fixed to the glue lam timber structure. In particular, the figures show the connection between the front steel plate and timber part of the structure - Fig. 5, the contact connection in a circle in the left. It also shows the connection of the steel tie, dia. 60 mm,, to the steel piece with clampings, Fig. 5 and 6.

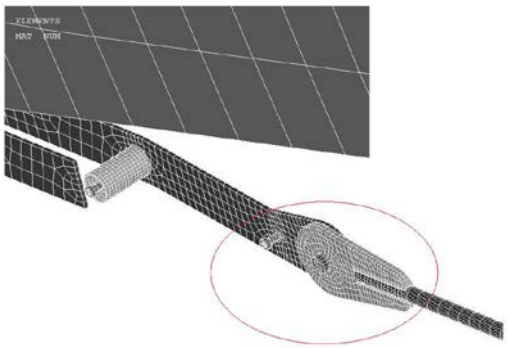

Fig. 6 Detail in the finite element grid: the tie

At the end of the steel tie there is a steel plate which is inserted into a steel piece which is, in turn, connected via a pin with a glue timber element

Fig. 7-10 show the resulting stresses obtained in ANSYS. The stress is measured in the direction which is parallel to the fibres and normal to the fibres. The 3D model in ANSYS shows also the shearing stress.

Such stress correlates with the stress measured in the beam model. The value in the circle in Fig. 11 is ca. 3.4 to 4 MPa in compression normally to the fibres. According to DIN 1052 the stress which the element is able to transfer is fc,α,d (the compressive strength normally to the fibres is ca 3.40MPa). The σ stress of the split compressive carrying capacity is 1.176. This means, the carrying capacity required by the standards was exceeded by ca. 18 per cent. The result of the numerical test correlates rather well with assumptions of the standard. The element, if compressed, is fully used up and needs to be reinforced (thread beams should be glued or full thread screws should bolted so that the compressive carrying capacity could increase).

Fig. 7 shows the compressive stress which is parallel to the fibres in the point of the compressive contact steel plate. The detail is highlighted in a circle. The contact bearing plant transfers the compressive force of ca. 656 kN from the tie into the timber mass. At the edge of the timber, the compressive stress is ca. 12.2 MPa. This is a local increase in the compressive stress which is caused by deformation of the steel plate and, in turn, compression of the timber. This is also influenced by a sharp change in the timber/edge geometry (which influences quality of the numerical calculation). Such increase is, however, likely and within limits of calculated carrying capacity of the timber: ca. 16.6 MPa in compression.

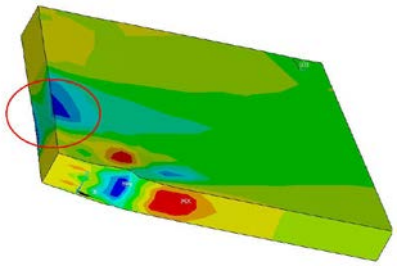

Fig. 7 Normal stress $\sigma_x$ [MPa] longitudinally with the fibres: NC41 combination

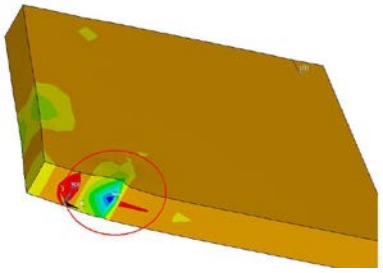

Fig. 8 Normal stress $\sigma_y$ [MPa] normal to the fibres: NC41 combination

Fig. 9 shows propagation of the shearing stress. In the circle, there are positive values of the shearing stress – they reach ca. 2.87 MPa. In the place where the glue lam beam is rotating the shearing stress is negative – ca. 3.51 MPa (there is a local extreme in the stress normal to the fibres as well as in the shearing stress). See Fig. 10.

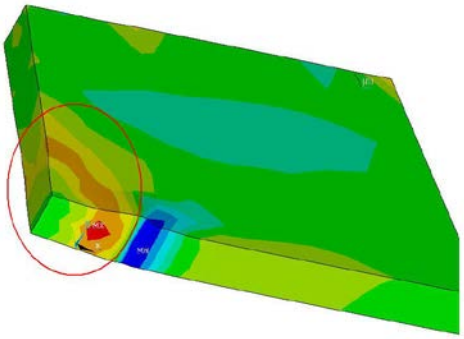

Fig. 9 Shearing stress $\sigma_{xz}$ [MPa]

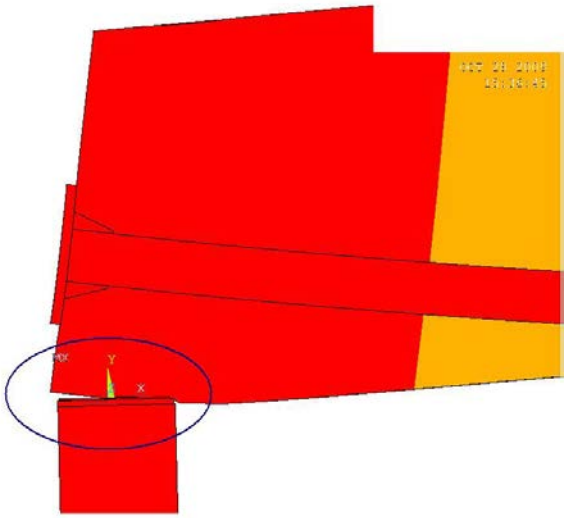

Fig. 10 Placing the beam on a reinforced concrete structure – deformation $u_y$ [mm]

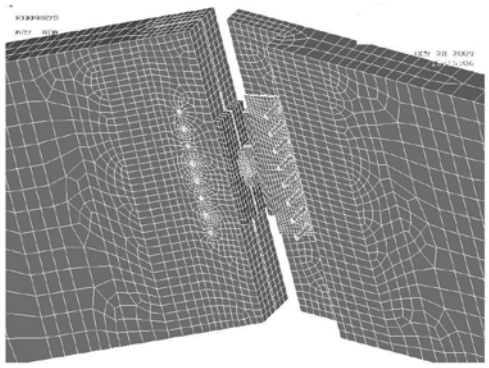

Fig. 11 Detail of the top connection

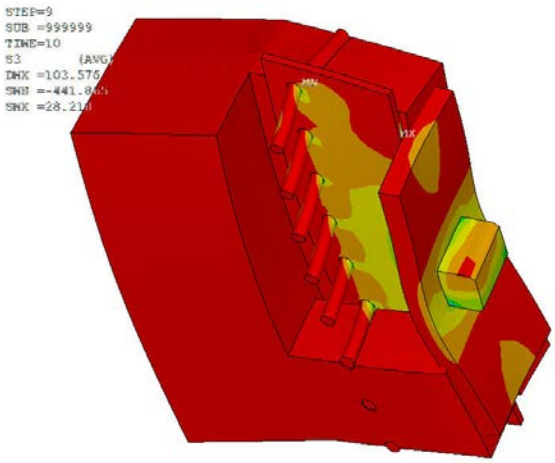


Fig. 12 Deformation of the top connection

Deformation of the detail in the vertical direction in the 3D model is ca. 120 mm, while deformation in the beam model is ca. 139 mm. That difference can be explained as follows: according to the standard applicable for calculation pursuant to the second order theory, the Eo modulus of elasticity is decreased in a beam model by gamma = 1.3. The modulus of elasticity, $E$, for calculation pursuant to the second order is the modulus of elasticity, $E_o$, divided by gamma.

This means that the glue lam structure is not so rigid and deformation in the beam model is rather high. A detail of the top connection has been modelled as well – see Fig. 11.

Fig. 12 shows transfer of deformation from the 3D frame into all elements of the steel joint as well as into the glue lam structure. The pins are plasticized and part of then have just started plasticizing.

The vertical force $V_z$ is by two orders lower than the horizontal force, $H_x$. See Table 2. The structure as a whole is loaded more or less symmetrically - the maximum horizontal force $H_x$ is in the top and the minimum vertical force $V_z$ is almost zero. See Table 2. Fig. 12 shows multiple deformation of the pin connection. It informs about the direction of deformation and shows the deformation against the original state without any deformation. The main compressive stress at pins for NC41 is 486 MPa. The original assumption based on a simplified manual design was that the top steep compressive plate takes over the complete horizontal force $H_x$ and transfers the force through the contact into the timber mass. In this model, however, the joint is so rigid (it is a welded plate for pins with the compressive plate) that $H_x$ is divided and applied through the steel plate into the timber as well as into the pin connection.


Fig. 13 Geometry + external bonds – top connection

This means that the connection can be evaluated as a whole in more detail. For the sake of completeness, information needs to be added about the modelling and boundary conditions for that numerical model in ANSYS. The pins were dia. 20 mm pins and the modelled drilling was 21 mm. The gap between the front plate and timber face was 0 mm.

In real structures, there are inaccuracies in installation of the pins (the drilling is often bigger) or the gap between the front plate and timber distance is bigger - even by several milimeters. Those impacts have not been modelled. This, however, may indicate that in case of minor inaccuracies the pin connection will deform will such a way that the front plate will be in contact with timber. This may happen only if the gap between the front plate and timber face is little only (and this should be checked in real structures). The pins will, anyway, deform and are subject to extra load. A partial solution would be to design an accurate connection so that no deformation could occur or to increase ductility of the pin connection (the steel pin starts plasticizing and local load of the timber in the place of connection will decrease – in particular, the tensile stress which is normal to the fibres will be reduced).

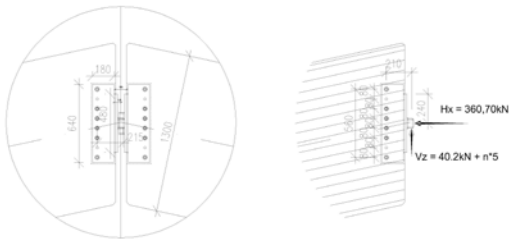


Fig. 14 Detail of the top connection + NC57 + *n*·5 combination

## IV. Analysing the Stiffness of the Top Purlin

This chapter analyses in detail the top connection. Attention is paid to re-distribution of strain on contact surfaces between the timber and steel sections and stiffness of the joints.

In order to model deformation accurately, the model of the top part is made for the NC57 and NC57 + n·5 combination. The model of the structure is taken from the previous model of the frame. The upper section of the connection was loaded by force in steps. Fig. 13 shows the external bonds in the top connection model as the fixing at the end of the LLD beam (the non-sliding bond in any direction). The load is simulated in steps as a load applied onto a pin. See Fig. 14.

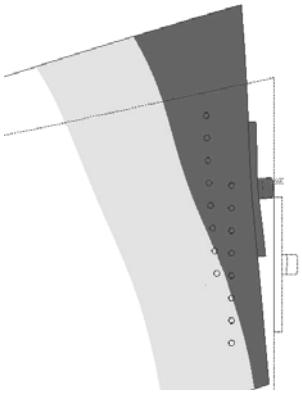

Fig. 15 Deformation of the joint

NC57 is the combination with the maximum vertical force which forces the joint to rotate. Deformations and forces applied onto the pin connection were investigated into and attention was paid to the general behaviour of the whole system. Fig. 15 shows the probable behaviour with deformation and deviation of the connection top. The connection is pressed in and rotates in a point where it is in contact with the timber part of the structure.

The NC57 + n·5 combination consists only from the loading combination which should represent the behaviour of the joint which is subject to the exceptional load when the vertical force, $V_z$, goes up, while the horizontal component of the load remains constant. The only purpose of the test is to check the behaviour of the model in limit load (the force loads for such load cases are at the very limit of the load-carrying capacity of the physical connection). In real structures of that type, such application is not possible.

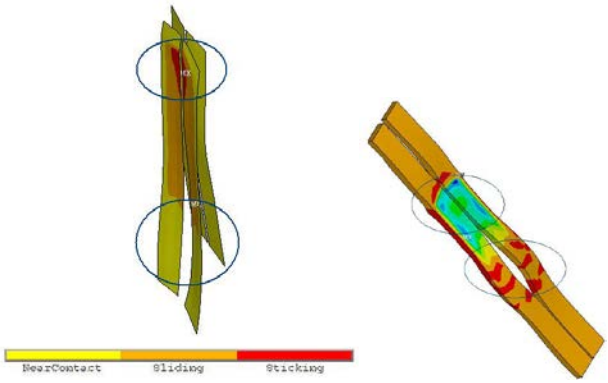


Fig. 16 ANSYS – deformation in a part of the top connection in NC57+*n*·5

Fig. 17 ANSYS – deformation of the steel top connection in NC57+*n*·5

The top part of the connection is loaded with NC57 + *n*·5 in two cycles. In the first cycle, the pin is loaded with the vertical force, $V_z$, from 0 kN to 40.20 kN and with the horizontal component, Hx, from 0 kN to 360.78 kN. When the structure is loaded fully with the load, the vertical force, $V_z$, starts increasing from 20.00 kN up to 353.30kN, while the horizontal component remains $H_x$, = 360.78 kN.

Considering the stiffness obtained pursuant to DIN 1052 and the values obtained in the numerical model, two additional models were prepared. The reason was to obtain detailed rotational stiffness of the top connection and to validate the values in several numerical tests. In the both models NC 07 and NC 08 the horizontal force, $H_x$, was neglected. In the last model, NC 07, the pressure plates at the timber front was removed. The purpose was to analyse the rotational stiffness of the steel joint and the influence of the horizontal components, $H_x$, and the front pressure steel plate on stability of the steel joint.

The data obtained in the ANSYS software are compared with assumptions 1 - 4 which are based on a simplified assumption of the joint connection. According to the simplified assumptions, the following boundary conditions are taken into account in order to maintain the linear relations (the material and deformation):

1. The horizontal force is transferred fully through the pressure contact between the timber and steel plate.

2. The vertical force is partly transferred by friction between the timber - steel plate contact. The friction coefficient at rest is 0.2.

3. The steel pins are involved in stiffness as soon as the moment condition of balance towards the steel plate is not in balance (when the moment caused by the stabilising horizontal force $H_x$ to the edge of the steel plate equals to or is less than the moment cause by the vertical force, $V_z$).

4. The joint rotation consists of two components (the joint rotation = the rotational stiffness of the connection + rotation of the LLD structure as a whole)

For NC57 the joint is loaded with $H_x$ = 360.68 kN and $V_z$ = 40.80 kN. In this situation which occurs in the real NC57 combination the deformation and forces occur in the area specified in the standards (more or less in elastic areas, out of the pin area – according to the standards, the joint should be ductile and certain strain and softness of the steel connection is required. This will eliminate local application of high forces into a "rather soft" timber and distribution of forces to other fasteners in the assembly group). The stress in pins is ca. 374 MPa. In the timber sections, the compressive stress is ca. 22 MPa and runs parallel with fibres. When selecting the grid and boundary conditions, the values of stress in the elements are not quite detectable but are still within limits of the acceptable assumptions.

Fig. 16 – 17 shows the NC57 + 5·*n* combination where the connection is loaded with the vertical force, $V_z$, which ranges from 0 to 353.30 kN. The connection is also loaded with the horizontal constant force, $H_x$ = 360.68 kN. The compressive stress for the pins is 648 MPa there and the steel joint deviates considerably from the front of the timber structure in Fig. 17. While the entire surface in the simplified assumption was the steel - timber contact, in this case the vertical force of ca. 353 kN causes the steel plate to deform and both the vertical component $V_z$ and the horizontal component $H_x$ result in considerable strain in the pin joint.

If one uses the original equations in [14] and [15], the final force at the furthest pin is 51 kN. That force exceeds the load-carrying capacity of the pin. (In reality there is still a ca. 50 per cent safety margin for short-lasting loads in a pin connection against the standards. The compressive stress of 648 MPa is, however, at the very limit of real acceptability for the pin. The measured load-carrying capacity for the pin is between 540 - 670 MPa and the steel plasticizes without any safety margin with such values). The angle between the vectors of forces caused by the moment and the shifting force is β = arctg(FV/FM) = 60° (in that case, the model is simplified in distribution of forces, the maintained centre of gravity, elastic behaviour...). If the final angle is compared graphically with Fig. 17, the conclusion is that the direction and, to a certain extent, the magnitude of deformation are approximately in line with the calculated value: β = 60°. In that case, the shifting force plays the decisive role in deformation of the pin connection. But there is also horizontal deformation caused by the moment from the vertical $V_z$. The moment conditions for balance towards the upper edge of the steel plate are $M1$ = 85.56 kNm and $M2$ = 24.73 kNm. If $M1 > M2$, the top steel plate will not rotate (the pins should theoretically transfer only $V_z - V_{ft}$ which means that the fiction force equals to $H_x$·0.2 which is ca. 360·0.2 = 72 kN). It is clear that the links and relations between the stiffness and sections of the structure influence each other so much that the pin connection is loaded from the very start with both rotation and the shifting force. The results can be used to model the approximate rotational stiffness of the connection. The simplified value for the pin connection, $K_{\varphi II}$ = 4 MNmrad$^{-1}$, is really only approximate. In reality, the stiffness is influenced also by the front steel plate and the balance is influenced probably by $H_x$ (which is of a rather stabilising character, in that case).

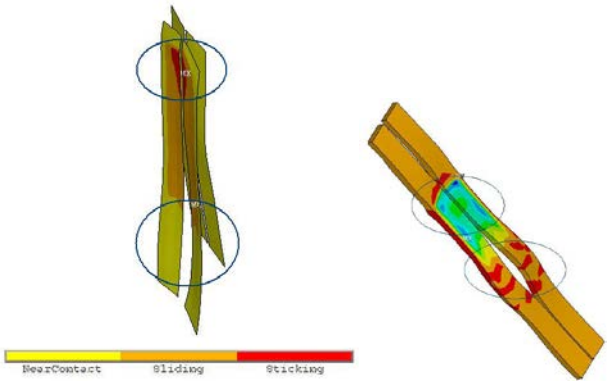


Fig. 16 ANSYS – deformation in a part of the top connection in NC57+n·5

Fig. 16 shows results for the contact surfaces. Three colours from the colour scale represent the status of contact in the contact surfaces. The colour in the left shows a close contact, while the middle colour indicates slippage. The colour in the right bottom corner means clear and full contact between the surfaces.

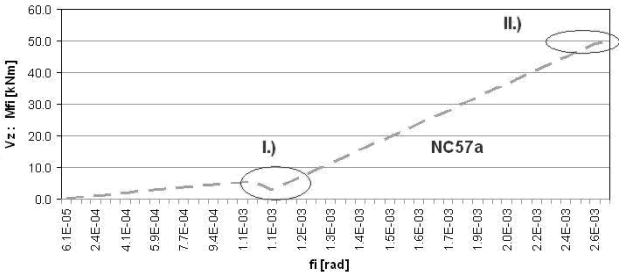


Fig. 18 Stiffness in the top connection: NC57 + n·5

Fig. 14 shows geometry of the steel joint. The rotational stiffness is calculated from the geometry. Influence of stiffness of the front steel plate is not taken into account. The values of the stiffness were considered without considering the duration of load and safety coefficient. This means, the values are approximate only.

Fig. 17 shows the compressive stress for the glue lam structure which runs parallel with the fibres: ca. 9 MPa. This figure shows a part of the timber structure only. The left top circle shows the pressure zone caused by the front pressure steel plate. The right bottom circle shows the force in the bottom pins which is caused by the moment of the vertical force $V_z$. That force attempts to open the joint towards the outside from the inside steel plate. According to the standards, bolts or full-thread screws should be installed there (in order to underpin the area which is subject to tension). Fig. 16 and 17 prove the assumption: the contact surface between the steel and timber recedes with the increasing vertical force $V_z$.

Fig. 18 shows the gradual loading of the connection in NC57 + n·5. A branch there represents the stiffness of the connection. An abrupt jump in the rotation, ca 1.10e-3 to 1.20e-3, is caused by changes in the load ($H_x$ remains at the full value of 360.69 kN, while the vertical force $V_z$ starts increasing there from ca 20 to 353 kN).

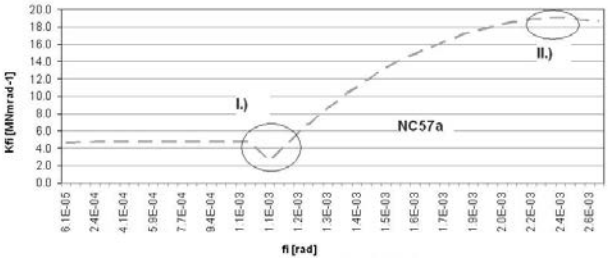


Fig. 19 Stiffness in the top connection: NC57 + n·5

Fig. 19 shows the gradual loading of the connection in NC57 + *n*·5. A branch there represents the stiffness of the connection which depends on the rotation. In order to save space in the chart, NC57a is used there instead of NC57 + *n*.5. The rotational stiffness is almost constant for the rotation from $6.10e^{-5}$ to ca $1.20e^{-3}$. The reason is the high horizontal force Hx and the relatively negligible vertical force $V_z$. That area is valid for NC57. In further loading steps, the rotational stiffness increases gradually until ca. $2.4e^{-3}$ is reached at the horizontal axis. Once this point is reached, the rotational stiffness starts decreasing.

The reason is probably plasticizing of the pin connection and pressure marks in the timber. For such strain, the vertical force cannot increase in such a way in reality - that branch is theoretical only.

Then the rotation of the glue lam structure as a whole was subtracted from the rotation above. The calculation was done for rotation on a cantilever in Fig. 13 using an integral which describes the rotation at the cantilever end caused by the force ($V_z$ and $H_x$).

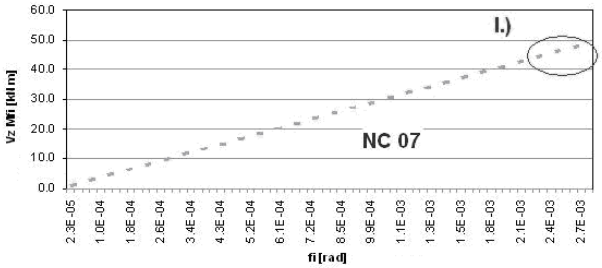


Fig. 20 Stiffness in the top connection in NC57 + *n*·5 loaded with $V_z$ only

Fig. 20 shows the gradual loading of the connection in NC07. A branch there represents the rotational stiffness of the connection which depends on the rotation. The structure was loaded only with the vertical force $V_z$. $V_z$ was calculated up to ca. 347 kN. The rotational stiffness is calculated as $K_\varphi = M/\varphi$. Using the equation above, the maximum rotational stiffness is ca. 35 $MNmrad^{-1}$, while the minimum stiffness is 17.43 $MNmrad^{-1}$. For the last steps in iteration when the vertical force is ca. 347 kN, the steel plate has almost no contact with the timber: it almost slides only on the timber structure.

In spite of this, the steel plate slightly stabilises the connection. This means, the rotational stiffness of the connection is slightly higher there than that of the connection where the influence of the front steel plate pressure is not taken into account.

Regarding the rotation, the difference in dislocation was measured at the *x* axis for the upper and lower points in the steel pressure plate. The final difference between the upper and lower dislocations in the *x* axis was divided by the distance of those points at the z axis (the height of the steel plate). Then the rotation of the glue lam structure as the whole was subtracted from the rotation above. The calculation was done for rotation on a cantilever caused by the force ($V_z$).

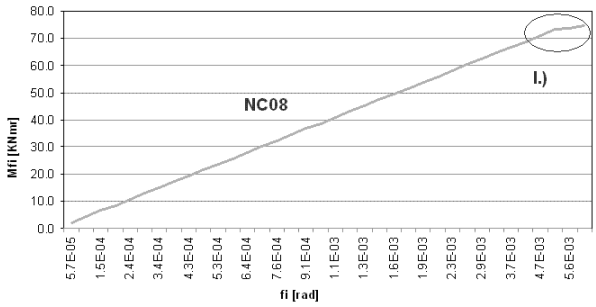


Fig. 21 Stiffness in the top connection in NC57 + *n*·5 loaded with $V_z$ only

Fig. 21 shows the gradual loading of the connection in NC08. A branch there represents the rotational stiffness of the connection which depends on the rotation. The structure was loaded only with the vertical force $V_z$. $V_z$ was calculated up to ca. 347 kN. The rotational stiffness is calculated as $K\varphi = M/\varphi$. Using the equation above, the maximum rotational stiffness is ca. 45 $MNmrad^{-1}$, while the minimum stiffness is 12.71

$MNmrad^{-1}$. That connection is loaded with the vertical force only $V_z$ and the influence of the contact steel plate on the timber front is not taken into account.

At the beginning of the loading process, the rotational stiffness in the connection is higher than that in the connection with the contact front steel plate. When the loading process continues, the rotational stiffness approaches the value of ca. 12.71 MNmrad-1 faster. The reason is, probably, that there is not any contact steel plate in the final phase of deformation which would change deformation in the connection which would, in turn, increase the rotational stiffness of the connection.

Regarding the rotation, the difference in dislocation was measured at the *x* axis for the upper and lower points in the steel pressure plate. The final difference between the upper and lower dislocations in the *x* axis was divided by the distance of those points at the *z* axis (the height of the steel plate). Then the rotation of the glue lam timber structure as the whole was subtracted from the rotation above. The calculation was done for rotation on a cantilever caused by the force ($V_z$).

The mentioned values of the rotational stiffness are really approximate only and a physical test must be carried out in order to validate them. According to the standard, the rotational stiffness is ca. $K_{\varphi II}$ = cca 4 $MNmrad^{-1}$ for the second limit condition of that connection. In general, the rotational rigidities which are calculated by means of the numerical methods are highly than the conservative values obtained pursuant to the standards.

The numerical models do not take into consideration the factor of time, fluctuation of humidity, inaccuracies in the connection and cyclical load of the connection (decrease in the stiffness) which provide higher values than those which are set forth in the standards. Therefore, each numerical model needs to be validated by a physical test. Only then the numerical model can be adjusted in order to describe the real loading response of the structure.

## V. Conclusions

The comparison calculations have proved that deformation in the structure correlates rather well with the force load (no physical test has been, however, carried out with respect to the deformation as perceived by us).

If material properties and contact elements are well chosen for the connection, the deflection of the structure is close to the value which has been in the models (the beam model or the volume model).

Considering the grid density, the stress in points of connection is within the load-carrying capacity of the timber. The stress in main elements is almost identical with the stress found pursuant to SCIA in a beam model.

The comparison calculations have proved that deformation in the structure correlates rather well with the force load (no physical test has been, however, carried out with respect to the deformation as perceived by us).

The maximum force which would be needed in order to break stability of the front contact plate which would lose the surface contact with the underlying timber structure is much higher than the values obtained by regular loads in the structure pursuant to the standards.

When using the contact elements, it is also necessary to consider the influence of the boundary conditions, grid density and grid quality, internal parameters of the contact elements and, in particular, the normal stiffness as all those factors play the role in the final stress. If the contact elements are used, the deformation and, in turn, the stress in the model can be described in a more realistic way.

This has been investigated in a rather small model where the purpose was only to find the contact stress in contact surfaces. The numerical model will be adjusted in computational models which will be dealt with in future works.

The main aim of this paper was to use contact elements. They were defined in surfaces in a 3D computational model. In ANSYS it is possible to define as many as 11 real constants in basic settings.

The parameters are based on physical properties of contact surfaces or they are parameters of the applicable numerical methods. The numerical method parameters influence, in particular, the manner of calculation convergence. The setting of the normal contact stiffness influences considerably the calculation convergence. In order to reach reasonable convergence, the normal stiffness of the contacts should be 1-2. If the normal stiffness is higher, more time is needed to reach the calculation convergence and results should be more precise. For certain tasks the stiffness might be less than 1. This is the case of tasks with demanding convergence when accurate penetration and size of constant stress are not needed. In the specified computation model the calculation has converged well for the initial value. It is also recommended to consider the factor of friction between the surfaces. The initial friction for steel-steel (0.1-0.2) or timber-timber (0.4-0.5) needs to be adjusted in order to reflect the real surface treatment. The use and setting of the contact elements is, however, different for each task. The reason is that the calculation's response is sensitive with respect to physical input parameters which are not known, frequently, in time of calculation. The reason is also that the use of the constant elements is influenced by the computational model, the finite element grid as well as by the type of the finite element.

## References

[1] ČSN 73 1702 mod DIN 1052:2004 Design of timber structures - General rules and rules for buildings. Praha, ČNI. 2007.

[2] ČSN EN 1995-1-1 (73 1701) Eurocode 5: Design of timber structures - Part 1-1: General - Common rules and rules for buildings. Praha, ČNI. 2006.

[3] D. Mikolasek, J. Brozovsky, O. Sucharda. "Analysing Effects of the Timber Structure Anchoring on Redistribution of Reaction and Eigen Frequency of the Structure," *In Proceeding of the international conferences: AMATH'13,* Budapest, Hungary, WSEAS Press, 2013, pp. 222-229.

[4] I. Furdui, D. Diaconu, "CFRP Strengthening of Glued-Laminated Timber Beams Experimental results," *In Recent Advances In Civil And Mining Engineering, Proceedings of the 4th European Conference of*

*Civil Engineering (ECCIE '13), Proceedings of the 1st European Conference of Mining Engineering (MINENG '13)*, Antalya, Turkey October 8-10, WSEAS Press, 2013. ISBN 978-960-474-337-7

[5] M. Karmazínová, Actual Stresses in CFRP-Reinforced Composite Timber Beams. Recent Researches in Environmental And Geological Science. Kos Island, Greece July 14-17, WSEAS Press, 2012, ISBN 978-1-61804-110-4

[6] A. Ceccotti, *Timber–concrete composite structures*. H. Blass (Ed.), Timber engineering-step 2, Centrum Hout, The Netherlands, 1995.

[7] Z.W. Guan, E.,C. ZHU, "Finite element modelling of anisotropic elasto-plastic timber composite beams with openings," Engineering Structure, Vol. 31, 2009, p. 394-403.

[8] XinWu Wang, "Nonlinear finite element analysis on the Steel Frame with semi-rigid connections," In *7thWSEAS International Conference on Applied Computer and Applied Computational Science*, China, April 6-8, 2008, pp. 31-35.

[9] S. Boljanovic, S. Maksimovic, I. Belic, "Total fatique life of structural components," *In Proceedings of the 2nd WSEAS International Conference on Applied Computer and Theoretical Mechanics*, Italy, November 20-22, 2006, pp. 1-6.

[10] P. Kuklík, A. Kuklikova, "Methods for evaluation of structural timber," *Wood Research*, Vol. 46, 2001, Iss. 1, pp. 1-10, ISSN 0012-6136.

[11] A. Lokaj, "Timber Beam Reliability Assessment," *In Euro-SIBRAM 2002*, Collloquium, Praha: ITAM CAS, 2002.

[12] K. Vavrusova, "New alternative methods for design of joints and elements of timber structures". *In 3rd International Conference on Civil Engineering, Architecture and Building Materials, CEABM 2013, Applied Mechanics and Materiále*, Vol. 351-352, 2013, Pages 1710-1713.DOI: 10.4028/www.scientific.net/AMM.351-352.1710.

[13] M. Krejsa, P. Janas, R. Cajka, "Using DOProC Method in Structural Reliability Assessment." *In ICMAM2012, Applied Mechanics and Materiále*. Vol. 300-301 (2013), pp. 860-869 (10 p). ISBN 978-3-03785-651-2.DOI: 10.4028/www.scientific.net/AMM.300-301.860.

[14] B. Koželouch, "Design, calculation and assessment of wooden constructions," (In Czech: Navrhování, výpočet a posuzování dřevěných stavebních konstrukcí, Obecná pravidla pro pozemní stavby, Komentář k ČSN 73 1702:2007). Praha: ČKAIT, 2008, ISBN 978-80-87093-73-3.

[15] B. Koželouch, "Timber structures Eurocode 5, STEP 2, detail design and structural systems," (In Czech: Dřevěné konstrukce podle EUROKÓDU 5, STEP 2, Navrhování detailů a nosných systémů). Zlín: KODR, 2004, ISBN 80-86 769-13-5.

[16] B. Straka, "Design of Timber Structures," (In Czech: Navrhování dřevěných konstrukcí). Brno: CERM, s.r.o., EXPERT Ostrava, 1996. ISBN 80-7204-015-4.

[17] K. Becker, K. Rautenstrauch, "Ingenieurholzbau nach Eurocode 5, Konstruktion, Berechnung," Ausführung. Ernst & Sohn, 400 p., 2012, ISBN 978-3-433-03013-4.

[18] R. A. Gunderson, J.R. Goodman, J. Bodig, "Plate Tests for Determination of Elastic Parameters of Wood," *Wood Science*, Vol. 5., p. 241-248, April 1973.

[19] A. Lokaj, K. Klajmonova, "Round timber bolted joints exposed to static and dynamic loading," *Wood Research*. Vol. 59, Iss. 3, 2014, p 439-448.

[20] H. Johnsson, "Plug Shear Failure in Nailed Timber Connections - Avoiding Brittle and Promoting Ductile Failures," Doctoral thesis, Div. of Timber Structures, Luleå University of Technology, 2004.

[21] Scia Engineer [online]. 2012 [cit. 2012-01-01]. WWW: < http://www.scia-online.com>.

[22] O. C. Zienkiewicz, *The Finite Element Methode in Engineering Science*. McGraw- Hill: London, 1971.

[23] RELEASE 11 DOCUMENTATION FOR ANSYS, SAS IP, INC., 2007.